

SPACE DEBRIS IN EARTH ORBIT: CAUSES AND CONSEQUENCES

ditps://doi.org/10.56238/sevened2025.011-075

Jean Paulo dos Santos Carvalho¹, Valéria Santos Corbacho²

ABSTRACT

From the launch of the first artificial satellite around the Earth to the present date, several non-functional objects are orbiting the planet, called space debris. In this work, we investigate ways to mitigate space debris to contribute to the sustainability of space exploration. To do this, we analyzed the 2022 ESA report where we present the main data on the evolution of space debris. We present mathematical modeling of major orbital perturbations and perform numerical simulations to show the orbital evolution of space debris. The idea is to encourage sustainable missions and measures to address the global problem of space debris.

Keywords: Space debris. Sustainability. Orbital disturbances. Satellite.

² Master in Astronomy State University of Feira de Santana https://orcid.org/0000-0003-4181-891X

¹ Dr. in Physics Center for Science and Technology in Energy and Sustainability Federal University of Recôncavo da Bahia State University of Feira de Santana https://orcid.org/0000-0002-1979-3739



1 INTRODUCTION

Much of contemporary life is dependent on the technological apparatus sent and established in the orbit of our planet. It is from this technology that we monitor climate change and create communication and navigation systems, in addition to helping the evolution of science. However, all of these services derived from this technological apparatus may be constantly threatened with being destroyed by the growing number of space debris – nonfunctional objects that are orbiting the Earth. Since the beginning of the space age, 1957, there has been more space debris in orbit than operational satellites. More precisely, space debris is defined as all artificial objects, including fragments and elements thereof, in orbit around the Earth or reentering the atmosphere, which are not functional (IADC, 2002 apud ESA, 2022, p. 10). These objects are also called space junk.

The problem of space debris was first publicized in the early 1960s by the United States, but only in 1978, when Donald Kessler (KESSLER AND COUR-PALAIS, 1978) warned of the danger of collisions and explosions of space debris in orbit, which could cause a chain reaction (Kessler Syndrome) and make spaceflight very dangerous. It was that the international scientific community became aware of the issue of debris. The first conference organized by the American Space Agency (NASA) took place in 1982, with the theme focused on space debris, after which some other conferences and meetings led to the creation of the "Inter-Agency Debris Committee" (IADC) in 1993, initially founded by the following space agencies: ESA (Europe), NASA (USA), JAXA (Japan) and Roscosmos (Russian Federation). Subsequently, nine more agencies joined the IADC: ASI (Italy), CNES (France), CNSA (China), CSA (Canada), DLR (Germany), KARI (South Korea), ISRO (India), NSAU (Ukraine) and UKSA (United Kingdom). It is worth noting that space activities in Brazil are coordinated by the Brazilian Space Agency (AEB), which is an autarchy of the Ministry of Science, Technology and Innovation responsible for Brazil's space program.

The IADC was founded as a forum for technical exchange and coordination on space debris and today is regarded as the leading international technical body in the field of space debris. Space debris has also been a recurring agenda item on the agenda of the United Nations Scientific and Technical Subcommittee, Committee on the Peaceful Uses of Outer Space (UNCOPUOS) since 1994. In 2002, the IADC published its Space Debris Mitigation Guidelines, this document brings a series of rules on how to design, launch and dispose of space missions without polluting near-Earth space. The guidelines established by the IADC initiated proposals for decongestion of the orbit and were the basis for space policies aimed at this purpose in the last 20 years. To get an overview of global debris mitigation efforts and raise awareness about space, since 2016, the European Space Agency (ESA), has been



publishing annual Space Environment reports (see, for example, ESA, 2022) updating on what has been happening in the near-Earth space environment and what has been done to make it sustainable in the long term. Some of the objectives of the report are: to provide a transparent overview of global space activities; estimate the impact of these activities on the space environment; quantify the effect of internationally endorsed mitigation measures aimed at environmental sustainability. The reports are based on describing the space environment based on observable characteristics, such as: the amount of mass, area and count of objects passing through different orbits, with greater emphasis on orbits: low (LEO) and geostationary (GEO). The report also identifies the most internationally accepted space debris mitigation measures, such as: payloads and rocket bodies should not release, or minimize as much as possible, space debris during normal operations; minimization of the potential for disruptions in orbit; avoid and/or eliminate the permanent or periodic presence of space debris primarily in low Earth orbit (LEO) and geostationary orbit (GEO); and collision avoidance in orbit. The use of these space debris mitigation measures can make sustainable forms of space operations possible, especially when we look at the Earth's orbital environment as a finite resource, so the international adoption of these measures can lead to a future in which space debris is not a problem. Otherwise, space debris could even derail space missions.

Several studies are being developed on space debris mitigation. For example, in Gkolias and Colombo (2019) the authors begin by describing the growth of space debris in geostationary orbit (GEO) and highlight that in the 90s the first discards were sent to the graveyard orbits used to avoid increasing the probability of collisions between satellites in the GEO region. The graveyard orbit is a disposal region that aims to increase the altitude of perigee by about 235 km and place space junk in a nearly circular orbit above the GEO region. One observation we make here is that the use of graveyard orbit will not decrease the probability of debris colliding and the return of these objects to the GEO region, but it is a mitigation solution anyway. In Formiga et al. (2019) the authors comment on the danger of debris clouds formed by small particles or fragments generated due to explosions of natural or artificial bodies, where they studied the evolution of the parameters as they approach the Earth, as each fragment will have different eccentricity and semi-major axis values. The idea was to map and analyze the different trajectories of this new distribution of space elements by calculating the orbital variations of each fragment of the cloud, after calculating the density it is possible to establish the average number of collisions, determining the possible risks of collisions with space vehicles and the maneuvers necessary to avoid it.

In Carvalho et al. (2021), the authors draw attention to the impacts and dangers that space debris can cause both to society and space exploration, they also present proposals



to solve this problem with the advancement of technology. The authors make a comparison of the increase in debris based on ESA reports from the years 2017, 2018 and 2019. In Carvalho et al. (2022) a solar sail is considered as a form of space debris removal, which is a technology that opens up new and challenging possibilities for space science missions, such as deep space exploration, space debris removal strategies, and long-period missions in the solar system. Solar sail is a type of propulsion that uses the pressure of solar radiation to generate acceleration, gains momentum by reflecting photons. The authors analyze the orbital evolution of space debris considering the main disruptive forces and a solar sail attached to the debris. They also develop a mathematical model for solar radiation pressure (PRS) in which the disturbing body is in an elliptical and inclined orbit. In Früh and Jah (2014) the authors consider the strength of the radiation pressure to analyze the area/mass ratio, the actual effective area that is exposed to the Sun, the reflection properties and the orientation of this effective area. In Casanova et al. (2015) an analytical and numerical model is developed to propagate space debris in terrestrial geostationary orbit. The authors found that for large values of the area/mass coefficient, PRS is the most important disturbance. It was also found that the J2 effect due to the flattening of the Earth, the effect of the Sun and the Moon as disturbing bodies, are the close, in order of magnitude in the dynamics studied. The application of the model used allows the propagation of debris that can remain in orbit for thousands of years because of the eccentricity of the geostationary orbit, which has an order of magnitude of about 10-2, and is not influenced by the effect of atmospheric drag caused by the gases that form the Earth's atmosphere.

In Kelly et al. (2016) it is shown that it is plausible to exploit the natural effect of PRS to maneuver space debris in GEO orbit. Causing the displacement of these objects into the graveyard orbit near the GEO region. For this there would be a need for a control system to ensure that the debris is placed in this graveyard orbit. In Ferreira (2019), Lima (2019) and Gonçalves (2021) the authors studied the theme of space debris, in particular, analyzing the orbital evolution of debris considering the main orbital perturbations. Highlighting that the solar sail was taken into account to amplify the growth of eccentricity and thus direct the debris to the Earth's atmosphere to be incinerated. It is well known that the removal of space debris is necessary to reduce the likelihood of collisions in orbit and reduce the potential for mission failure of active spacecraft, as commented on in Arshad et al. (2025). The authors did a vast review on space debris mitigation. Various active and passive methods have been analyzed to remove or deorbit space debris. Active methods include the use of tentacles, robotic arms, nets, tethers, harpoons, lasers, deorbiter modules, ion beam guides, foam-based methods, and sling-sat, while passive methods include the use of trailing sails and solar sails.

7

Thus, space debris is a problem that has an impact on space exploration, these objects can cause damage to artificial satellites operating in Earth orbit, and when they return to the planet, they can cause damage as a result of falling fragments in residential or industrial regions. The sustainability of the space environment is essential to ensure the exploration of Earth orbit efficiently and responsibly. The search for sustainability in all areas of the exploration of environmental spaces is currently an essential theme for the success of any technological enterprise that seeks economic and scientific development. Sustainability holds a broad concept that must be applied to the space exploration environment. The Brundtland commission defined Sustainable Development as (CASSEN, 1987, p. 16).

(...) one that satisfies the needs of the present without compromising the ability of future generations to satisfy their own needs.

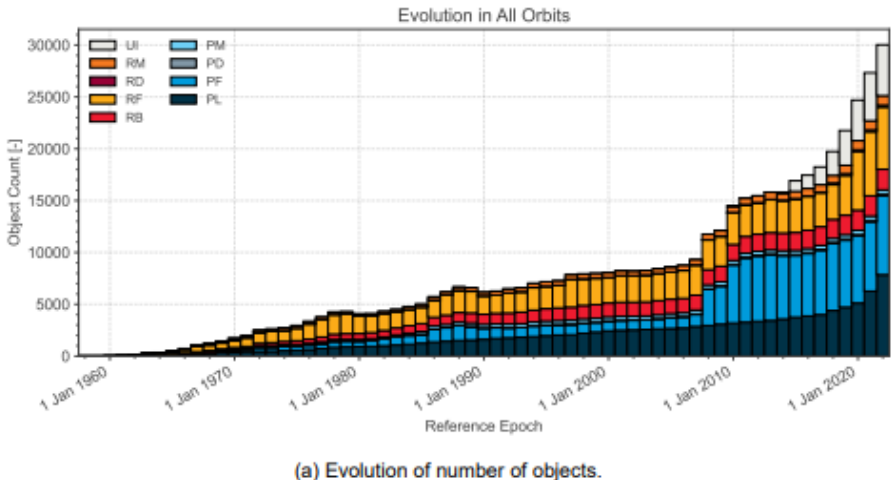
When the exploration of space respects the principle of sustainable development, it ensures the effective and lasting use of the space environment. In order for us to continue to benefit from the advances in technologies present in space in the future, it is necessary to use the space environment in a sustainable way, investing in technologies for the mitigation of space debris in order to explore the sustainable space environment.

2 SPACE DEBRIS NUMBERS

According to ESA (2022), the number of space debris is currently very large, and its accumulation does not stop growing and congesting Earth orbit. It is estimated that there are approximately 30,000 space debris tracked in Earth's orbit. The evolution in years of these cataloged objects in orbit is represented in Figure 1. The data is subdivided based on the classification of objects and orbits. Figure 1 shows that from 2020 onwards the number of objects around the Earth has grown considerably, in particular, due to the launch of large constellations of small satellites sent into space by private companies.



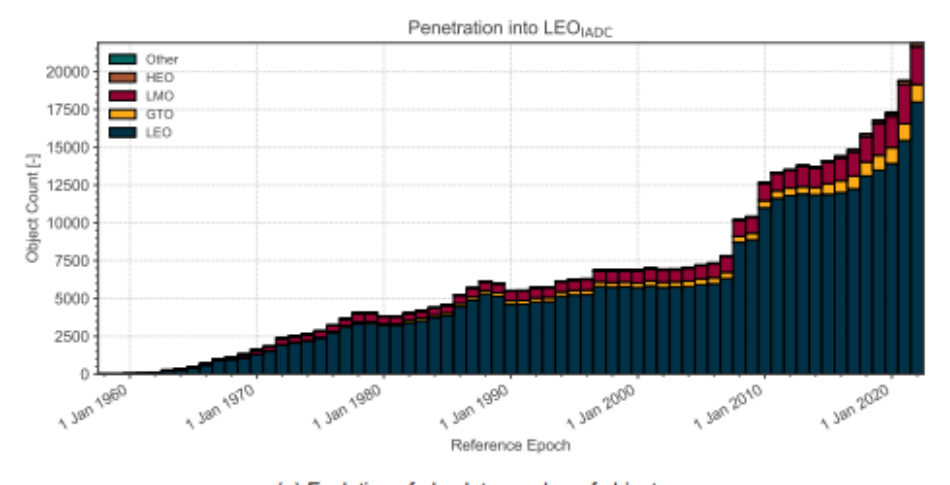
Figure 1 – Evolution of the number of objects orbiting the Earth.



Source: ESA (2022).

Regarding the LEO and GEO orbits, the absolute and equivalent number of objects interfering with these regions are represented in Figures 2 and 3. Figure 2 shows the evolution of the absolute number of objects residing in or penetrating the LEO orbit. Now, Figure 3 shows the evolution of the absolute number of objects residing in or penetrating Geostationary Orbit (GEO). Comparing Figures 2 and 3 it is possible to see the difference in the number of objects in these orbits. In LEO orbit (Figure 2) the number of objects is much higher than the number of objects in GEO orbit (Figure 3). This is due to the fact that the greater number of artificial satellites in operation in LEO orbit and also the discards of launch rockets. Adding the passage, through the LEO region, of other objects that are in higher orbits.

Figure 2 – Evolution of the absolute number of objects in LEO orbit.



(a) Evolution of absolute number of objects.

Source: ESA (2022).

The ESA report (2022) highlights the growth in the number of launches since 2020, mainly due to the creation of satellite constellations, which has made launches not only more



intense, but also more compact, as several satellites are launched at the same time and most of them have a mass of 100 to 1,000 kg. These actions greatly influenced the reduction of launch costs, but also made it more complex to monitor these objects individually, in addition to increasing the number of satellites and consequently space debris, especially in low Earth orbit, making it even more congested. As a result, according to ESA (2022), in recent years encounters between active satellites and debris, called "conjunctions", have also become more frequent, and this trend will be increasing, because, even though there is a growth in the proper disposal of inactive satellites and rockets used to launch satellites, there are still several of them adrift. For this reason, the report associates this unsustainable practice with the occurrence of Kessler Syndrome, in which the increase in the number of collisions could cause a cascade effect and compromise the sustainable use of space close to Earth.

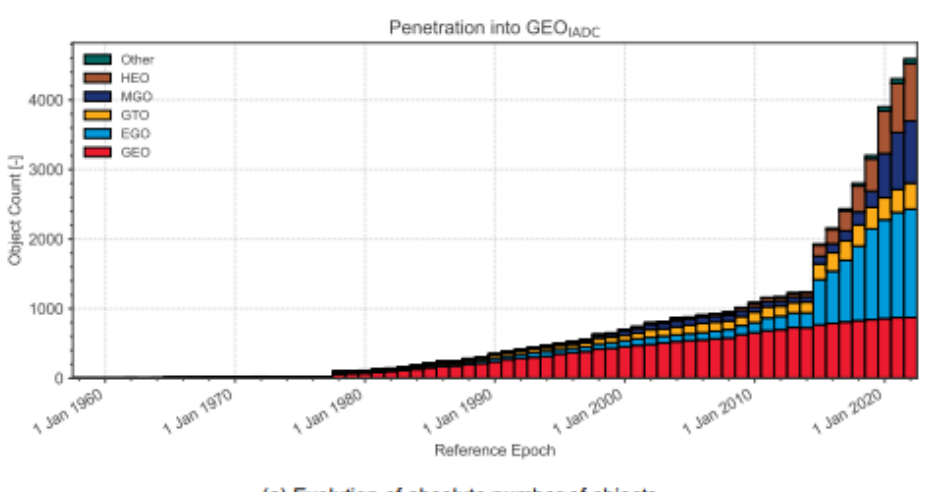


Figure 3 – Evolution of the absolute number of objects in the GEO orbit.

(a) Evolution of absolute number of objects.

Source: ESA (2022).

In conjunction events, alerts are issued that do not always indicate a fatal collision, but as the number of objects orbiting our planet has grown a lot over the years, an even more effective and automatic tracking system is needed, such as the one being developed by ESA (ESA CROSS - Collision Risk Assessment Software) to detect potential conjunctions with cataloged objects, capable of performing maneuvers to prevent collisions and reduce false alarms. It is worth noting that in addition to telescopes that observe the Earth's debris, there is also technology for observation from space, in which sensors on board artificial satellites in LEO are used to monitor objects in GEO (HU et al. 2016).

According to ESA (2022), the analysis presented in the reports has been systematically repeated annually since 2015. In the LEO orbit regime, in view of the increase in conjunction events in the space environment, and although today there is already a better awareness of



this problem, little has yet been done. If the mode of launch and disposal of space objects is not sufficiently sustainable, the number of collisions in Earth's orbital space will be unbearable and catastrophic in the future. For ESA (2022), the most viable alternative to alleviate this issue would be the standardization and execution of the mitigation guidelines already established by the IADC, where nations, institutions, and space agencies should comply with the standards already established, as well as start cleaning up near-Earth space. Attitudes that would avoid the increase of conjunctions and orbital congestion on Earth, ensuring the continuity of space exploration and satellite services. From the beginning of the space age to the end of 2021, there were 636 confirmed fragmentations in orbit, a summary of statistics on recorded fragmentation events is reported in Table 1. Post-mission disposal mitigation measures specifically aim to reduce the long-term interference of an object in the space environment, especially in LEO and GEO orbits. These measurements are associated with time criteria, i.e. so-called orbital lifetimes, and therefore require evaluating the long-term evolution of the orbits. For both orbits, different mitigation measures imply different end-of-life operations.

Table 1: Statistics on fragmentation events

Table 1. Statistics on fragmentation events.			
	The entire history	Last 20 years	
Number of events	636	246	
Non-deliberate events per year	9,5	11,7	
Annual rate of events where 50% of the generated shards have a lifetime of more than 10 years	2,8	2,6	
Annual rate of events where 50% of the generated shards have a lifetime greater than 25 years	1,9	1,7	
Average time (years) between release and fragmentation	5,5	10,2	
Average time (years) between release and fragmentation	1,0	6,8	

Source: ESA (2022).

Table 1 shows the number of objects of different sizes orbiting the Earth and their implications if a debris collides with a spacecraft. It is worth noting that the data was obtained by scientific models that estimate the total number of space debris objects in Earth's orbit. In this way, we can better understand the situation of the space environment and seek to solve the situation of space debris by seeking technologies that can make space missions sustainable. International space agencies have made an effort to disclose this data to show that the situation is really worrying and that we must pay attention to this problem before the







Chart 1 - Space junk in numbers

Chart : Oparo jamit in manuscro			
Number of objects	Size of objects	Implications	
		A collision would entail	
	lorger than 10 am	a catastrophic	
29.000	larger than 10 cm	fragmentation of a	
	(these are cataloged)	typical satellite.	
		A collision would	
		disable a spacecraft	
670.000	larger than 1 cm	and penetrate the ISS	
		shields.	
		A collision can destroy	
Mais de 170 milhões	larger than 1 mm	subsystems aboard a	
		spacecraft.	

Source: ESA (accessed on 07/16/2022)

https://www.esa.int/Space Safety/Clean Space/How many space debris objects are currently in orbit

3 END-OF-LIFE OPERATIONS IN LOW EARTH ORBIT (LEO)

Atmospheric drag is the most intense disturbance in the region of the LEO orbit, for this reason natural decay is the form of space debris re-entry and occurs most frequently in this orbit. A payload or rocket body operating in LEO orbit must limit its post-mission presence to a maximum of 25 years (ESA, 2022) from the end of the mission. However, this rule alone will not lead to a decrease in the amount of space debris, but it is an important step towards limiting the growth rate of space debris in LEO orbit. For cataloged objects, the orbital activity of a payload or rocket body can be calculated and the orbital lifetime estimated. Direct investigation (communication with the owners of the object) can be more efficient, but the request for data cannot always be answered, or not all owners can be identified, which ends up making the process of determining the end of the operational phase of an object even more difficult.

The methodology to determine the end of the operational phase of an object in LEO orbit requires much more than just orbit information, a statistical approach is required, which encompasses items such as: mission categorization and orbit control capability (CCO). The boundaries between having or not having CCO are not always well defined by technology. Because the effects observed by the space surveillance system may not be accurately distinguished in many cases. Impulsive maneuvers, multi-revolution use of electric propulsion, and large drag sail deployments are reliably picked up, and therefore objects exhibiting these characteristics are categorized as having CCO. The ESA report (2022) points out that there must be an assessment of the limitation of the useful life of satellites, according to the mitigation guidelines, the categorization of each object becomes fixed after 25 years. However, natural disturbances that interfere with the orbit of satellites can cause re-entry before this established period or missions that remove large pieces of space debris, in which case it should only be accounted for when such action is carried out. The relocations of the LEO orbit to orbits with a perigee altitude above 2,000 kilometers are no longer feasible at



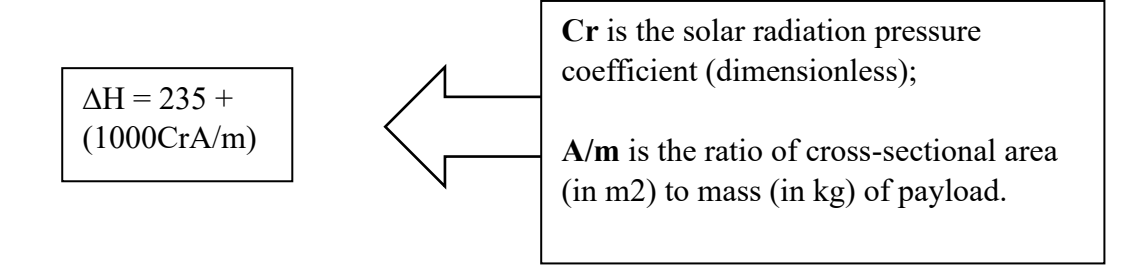
the end of the useful life of the satellites, this practice of debris mitigation does not guarantee sustainability in near-Earth space, as they must decrease in altitude over the years, returning to the initial situation.

4 END-OF-LIFE OPERATIONS IN GEOSTATIONARY ORBIT (GEO)

In Geostationary orbit, unlike what happens in LEO orbit, there is no natural mechanism that allows debris to leave this region. Although PRS is one of the most intense disruptive effects in this orbit (CASANOVA et al., 2015; VILHENA DE MORAES, 1981), there is not necessarily certainty as to the decay and re-entry of objects, once their usefulness has ended. The forecasts in this case are long-term and subject to uncertainties. It is known that debris in GEO orbit can remain for hundreds of years (CARVALHO et al., 2022; GKOLIAS AND COLOMBO, 2019 and references contained therein).

According to the ESA report (2022), a payload or rocket body operating in GEO orbit must be manoeuvred in a controlled manner during the disposal phase to an orbit that is completely outside the GEO Protected Region, avoiding congestion. Within the GEO orbit, the mitigation measure has been reformulated by the IADC, to ensure that disposal takes place in a graveyard orbit, for example, with minimal interference. For this to occur, at least one of the following two conditions must be met:

- The orbit has an initial eccentricity less than 0.003
- The orbit has a minimum perigee altitude ΔH (in km) above the geostationary altitude, according to the equation:



In addition to the disposal orbit having to have a perigee altitude sufficiently above the geostationary altitude, perturbation forces such as PRS, gravitational attraction, non-uniform mass distribution, among others, and resonance effects should not cause the payload and rocket bodies to return to the GEO protected region within 100 years. that is, in the long term. In summary, the release from geostationary orbit will be successful, if the criteria of the IADC formulation are met.



In this present work, based on the methodology presented in Carvalho et al. (2022), we considered the solar sail to amplify the growth of the eccentricity of a debris in the GEO region in such a way that the debris can approach the Earth's atmosphere to be incinerated.

5 MATHEMATICAL MODELING

In this section, we introduce mathematical modeling. We consider in the dynamics the main orbital perturbations on the orbital motion of space debris. Namely, the non-uniform distribution of the Earth's mass (flattening at the poles), the perturbation of the third cup (Sun and Moon) and the PRS. In celestial mechanics, the position of a natural or artificial celestial body is determined by the Keplerian orbital elements, there are six elements that are presented in Table 2.

Table 2 - Orbital elements

Symbols	Denomination	Define
а	Semi-major shaft	Shape and dimension
е	Eccentricity	Shape and dimension
Ω=h	Ascending node longitude	Position of the orbital plane in space
i	Inclination	Position of the orbital plane in space
ω=g	Perigee argument	Orientation of the ellipse in the orbital plane
t_0	Time of perigee passages	Satellite location on the orbital ellipse

Source: Prepared by the authors

The spacecraft's equation of motion is given by

$$\ddot{r} = \ddot{r}_T + \ddot{r}_{3C} + \ddot{r}_{PRS},\tag{1}$$

where r¨_T is the force induced by the Earth's gravitational field, the term r¨_3C is the result of the gravitational attraction of the third body (Sun and Moon) and the term r¨_PRS represents the acceleration generated by the PRS. From equation (1), the term r¨_T can be presented as the gradient of a given potential U_T which is written in terms of the vector position r of the spacecraft with respect to the central planet, as shown in equation (2):

$$\ddot{r}_T = \nabla U_T(\mathbf{r}),\tag{2}$$

rewriting equation (2) using known equations from Celestial Mechanics, in the simple mean model, to write the perturbing potential as a function of the orbital elements, after some algebraic manipulations we obtain equation (3), referring to the flattening at the poles of the central body (CARVALHO et al., 2022),

$$(3)\langle R_{J_2}\rangle = -\frac{1}{4}R_e^2 J_2 \frac{n^2(-2+3sen^2i)}{(1-e^2)^{\frac{3}{2}}},$$



where R_E is the Earth's equatorial radius, n is the average motion of the debris. The term due to the flattening of the Earth (J2) considered is the second zonal term of the geopotential. The term r_3C given in equation (1), can be written in the form (MURRAY AND DERMOTT, 1999)

$$\ddot{r}_{3C} = -\mu_{\odot} \left(\frac{r - r_{\odot}}{||r - r_{\odot}||^{3}} + \frac{r_{\odot}}{||r_{\odot}||^{3}} \right), \tag{4}$$

where is the gravitational parameter of the Sun and - is the vector in the direction of the probe towards the Sun. To represent the equation of the perturbation of the third body (Sun and Moon) as a function of the orbital elements, we again use the equations of Celestial Mechanics. This development is presented in Carvalho et al. (2022), in which the simple mean model is applied considering the third body in elliptical and inclined orbit, see Appendix A in Carvalho et al. (2022). Now, considering the term (PRS), in Tresaco et al. (2018) the acceleration exerted on a body perfectly reflected by solar radiation, expressed in equation (5), in the Oxyz inertial system, centered on the central body, described as: $\mu_{\odot} rr_{\odot} \ddot{r}_{PRS}$

$$\ddot{r}_{PRS} = -2P \frac{A}{M} \frac{r - r_{\odot}}{||r - r_{\odot}||} (5)$$

where - is the vector in the direction of the probe towards the Sun, and (A/m) is the areamass coefficient of the probe. The minus sign in equation (5) appears because the acceleration is opposite to the positive direction of this vector, and $rr_{\odot}P$, see equation (6), indicates the solar radiation pressure, given by:

$$P = \frac{I}{c}, \tag{6}$$

being the solar flux on the surface of the illuminated plane and *Ic* is the speed of light. The solar flux, equation (6), is defined as the amount of energy received on the surface of the illuminated satellite. Defined by (TRESACO et al., 2018)*I*

$$I = I_0 \left(\frac{1}{\rho}\right)^2. \tag{7}$$

The solar constant in 1 astronomical unit (AU) is 1358 W/m I_0^2 , and ρ is the average distance from the Earth to the Sun (1 AU). In Tresaco et al. (2016), equation (8) represents β , a dimensionless parameter that is the dimensionless ratio of the acceleration of the PRS in relation to the solar gravitational acceleration that measures the efficiency of the sail. Equation (9) characterizes the critical loading parameter for the Earth, and equation (10) corresponds to the sail loading parameter (area density) (TRESACO et al., 2018; MCINNES, 1999).

$$\beta = \frac{\sigma^*}{\sigma}, \tag{8}$$

$$\sigma^* = 1.53 \left(\frac{1}{\rho}\right)^2$$
,(9)



$$\sigma = \frac{m}{4}$$
 element. (10)

In terms of the Sun's luminosity, solar sail acceleration can also be described as: L_{\odot}

$$\ddot{r}_{PRS} = \frac{L_{\odot}}{c2\pi\rho^2} \frac{A}{m} (\boldsymbol{u_i} \cdot \boldsymbol{n})^2 \boldsymbol{n}, \tag{11}$$

equation (11), considering the stay of the candlestick in a fixed orientation perpendicular to the line of the Sun (||), $u_i n$ then the effect of the candlestick takes on its maximum value (·) $u_i n = 1$. Therefore, the candle loading parameter can be written as: $\sigma^* = L_{\odot}/c2\pi\mu_{\odot}$ Considering that the candle must maintain its orientation perpendicular to the Sun's line $n = \frac{1}{\rho} ||\rho||$ and the candle is located at a distance from the sun $\rho = ||r - ||$, the PRS is given by equation (12) (TRESACO et al., 2016): r_{\odot}

$$\ddot{r}_{PRS} = \beta \mu_{\odot} \frac{r - r_{\odot}}{||r - r_{\odot}||^3}$$
 (12)

thus, we can write the acceleration of the candlestick due to PRS as the gradient of the following potential:

$$U_{PRS} = -\beta \mu_{\odot} \frac{1}{||r - r_{\odot}||} \text{ element.}$$
 (13)

Disturbance due to PRS is directly dependent on the mass and size of the spacecraft and orbit altitude; In this way, we varied the area-mass and altitude coefficient of the satellite to observe the impacts generated in the sail dynamics. After algebraic manipulations and application of the simple mean model, equation (13) can be described as a function of the orbital elements, this development is presented in Carvalho et al., (2022), see their equation (22). The equation due to PRS is put into the form



$$\langle R_{SRP} \rangle = \frac{81}{27} \beta \frac{ean_{\odot}^{-2}a_{\odot}}{(1-e_{\odot}^{-2})^{2}} (-\frac{1}{27}(20\cos(i)-20)(\cos(i_{\odot})-1)(e_{\odot}^{2}-2/5) \times \cos(-l_{\odot}+g-h-g_{\odot}+h_{\odot}) - \frac{1}{27}(20e_{\odot}^{2}-8)(\cos(i)+1) \times (1+\cos(i_{\odot}))\cos(-l_{\odot}+g+h-g_{\odot}-h_{\odot}) + e_{\odot}^{2} \times (\cos(i_{\odot})-1)(\cos(i)-1)\cos(-3l_{\odot}+g-h-g_{\odot}+h_{\odot}) + e_{\odot}^{2}(\cos(i)+1)(1+\cos(i_{\odot}))\cos(-3l_{\odot}+g-h-g_{\odot}+h_{\odot}) + \frac{16}{27}e_{\odot}(\cos(i_{\odot})-1)(\cos(i)-1)\cos(-2l_{\odot}+g-h-g_{\odot}+h_{\odot}) + \frac{16}{27}e_{\odot}(\cos(i)+1)(1+\cos(i_{\odot}))\cos(-2l_{\odot}+g+h-g_{\odot}-h_{\odot}) - \frac{1}{27}e_{\odot}^{2}(1+\cos(i_{\odot}))(\cos(i)-1)\cos(-l_{\odot}+g-h+g_{\odot}+h_{\odot}) - \frac{1}{27}e_{\odot}^{2}(\cos(i_{\odot})-1)(\cos(i)+1)\cos(-l_{\odot}+g-h-g_{\odot}+h_{\odot}) + \frac{1}{27}e_{\odot}^{2}(\cos(i_{\odot})-1)(\cos(i)+1)\cos(l_{\odot}+g-h-g_{\odot}+h_{\odot}) + \frac{1}{27}e_{\odot}^{2}(\cos(i_{\odot})-1)(\cos(i)-1)\cos(l_{\odot}+g-h-g_{\odot}+h_{\odot}) - \frac{16}{27}e_{\odot}(\cos(i_{\odot})-1)(\cos(i)+1)\cos(2l_{\odot}+g-h+g_{\odot}+h_{\odot}) - \frac{16}{27}e_{\odot}(\cos(i_{\odot})-1)(\cos(i)+1)\cos(2l_{\odot}+g-h+g_{\odot}+h_{\odot}) - \frac{16}{27}e_{\odot}(\cos(i_{\odot})-1)(\cos(i)+1)\cos(3l_{\odot}+g-h+g_{\odot}+h_{\odot}) - e_{\odot}^{2}(\cos(i_{\odot})-1)(\cos(i)+1)\cos(3l_{\odot}+g-h+g_{\odot}+h_{\odot}) + \frac{1}{27}(20\cos(i_{\odot}-20)(e_{\odot}^{2}-2/5)(1+\cos(i_{\odot}))\cos(l_{\odot}+g-h+g_{\odot}+h_{\odot}) + \frac{1}{27}(20\cos(i_{\odot})-20)(e_{\odot}^{2}-2/5)(\cos(i)+1)\cos(l_{\odot}+g-h+g_{\odot}+h_{\odot}) + \frac{1}{27}(20\cos(i_{\odot}-20)(e_{\odot}^{2}-2/5)(\cos(i)+1)\cos(l_{\odot}+g_{\odot}-h_{\odot}+g+h) + \frac{1}{27}(20\cos(i_{\odot}-20)(e_{\odot}^{2}-2/5)(\cos(i)+1)\cos(l_{\odot}+g_{\odot}+g)+g_{\odot}^{2} + \frac{16}{27}\cos(-2l_{\odot}-g_{\odot}+g)e_{\odot}-1/27e_{\odot}^{2}\cos(-l_{\odot}+g_{\odot}+g) + \frac{1}{27}e_{\odot}^{2}\cos(l_{\odot}-g_{\odot}+g) + \frac{16}{27}e_{\odot}\cos(l_{\odot}-g_{\odot}+g) + \frac{16}{27}e_{\odot}\cos(l_{\odot$$

Note that the symbols with index represent the same orbital elements defined in Table 1, only they now represent the orbital elements of the Sun (or Moon), that is, the Earth's orbit around the Sun (or Moon). Being the average anomaly of the Sun (or Moon). $\odot l_{\odot}$

Considering the perturbations defined above, PRS (), the flattening due to $R_{PRS}J2$ (, the perturbations of the Moon () and the Sun (), the perturbing potential R_{J2}) $R_{Lua}R_{Sol}R$ is given by the sum of the equations of the orbital perturbations, described by

$$R = R_{Sol} + R_{Lua} + R_{PRS} + R_{I2}. (15)$$

By substituting the perturbing potential given by equation (15) into the planetary Lagrange equations (equation 16) and numerically integrating the system of nonlinear differential equations we obtain the results shown in the next section. We consider the



numerical integration method of Maple Software, "Fehlberg fourth-fifth order Runge-Kutta method with degree four".

$$\frac{de}{dt} = \frac{-\sqrt{1 - e^2}}{na^2 e} \frac{\partial R}{\partial g} + \frac{1 - e^2}{na^2 e} \frac{\partial R}{\partial M}$$

$$\frac{di}{dt} = \frac{-1}{na^2\sqrt{1 - e^2 \sin i}} \frac{\partial R}{\partial h} + \frac{\cos i}{na^2\sqrt{1 - e^2 \sin i}} \frac{\partial R}{\partial g}$$

$$\frac{dg}{dt} = \frac{\sqrt{1 - e^2}}{na^2 e} \frac{\partial R}{\partial e} - \frac{\cos i}{na^2 \sqrt{1 - e^2 \sin i}} \frac{\partial R}{\partial i}$$

$$\frac{dh}{dt} = \frac{1}{na^2\sqrt{1 - e^2 \sin i}} \frac{\partial R}{\partial i}.$$
 (16)

6 RESULTS

By numerically integrating equation (16) using the perturbing potential given by equation (15) via Maple Software, we obtain the variation of the orbital elements as a function of time. We consider here the numerical simulations to investigate the orbital behavior of an artificial satellite (Simulation 1) in operation and of two decommissioned satellite-type space debris (Simulation 2 and 3).

6.1 SIMULATION 1 - SATELLITE IN OPERATION

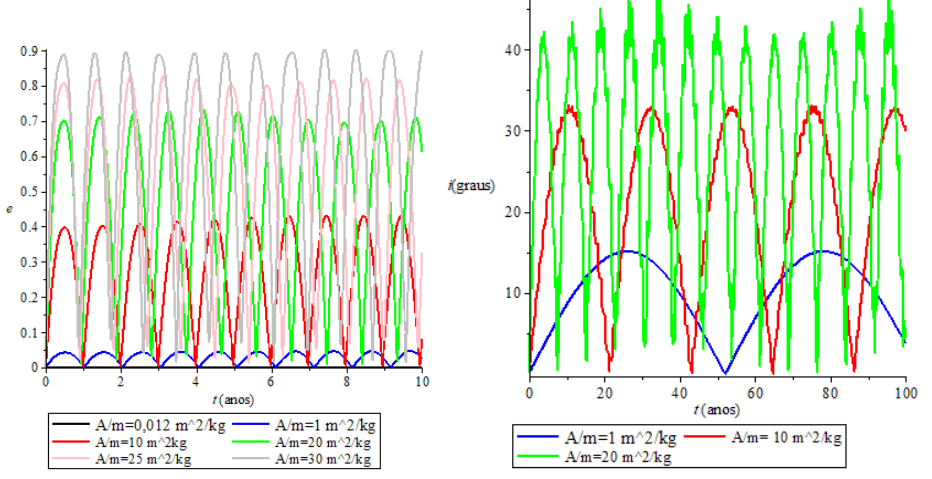
The Galaxy 30 (G-30) is an artificial satellite that has been placed in geosynchronous Earth orbit, it is part of Intelsat's Galaxy fleet. Orbital data were obtained from site https://www.privateer.com/. Orbital data: a=42165.8 km, e=0.0002, i=0.1640 degrees, $\Omega=85.9517$ degrees and w=34.3472 degrees, which corresponds to the orbit of a geostationary satellite. It is worth noting that when the eccentricity of a space vehicle grows over time, that is, the orbit becomes flatter and the vehicle tends to approach the surface of the central body or even collide with it. The area/mass ratio of a typical satellite is on the order of 0.012 m2/kg. Figure 4(a) shows that for a typical satellite the eccentricity practically does not vary over time (black curve), remaining stable for a long time. Now, when the opening of a solar sail is triggered to increase the area of the spacecraft, we notice that the larger the area, the greater the growth of the eccentricity (directly proportional). The effect of PRS is dominant in relation to other disturbances when a large area and small mass is taken into account. Therefore, PRS is



responsible for the growth of eccentricity causing the vehicle to approach the reentry region for the satellite to be incinerated in the Earth's atmosphere. In this way, it is possible to remove the satellite from the geostationary region at the end of its useful life in a sustainable way, as the propulsion used by the sail uses the source of energy from the Sun, which is a clean and abundant source of energy. However, there is a limitation of the technology to produce a candle with a very large A/m ratio, such as some values shown in Figure 4(a), to force the eccentricity to grow to high values. Note that Figure 4(b) shows that it is possible to amplify the slope growth to lower values of the A/m ratio, but for a longer time interval than Figure 4(a).



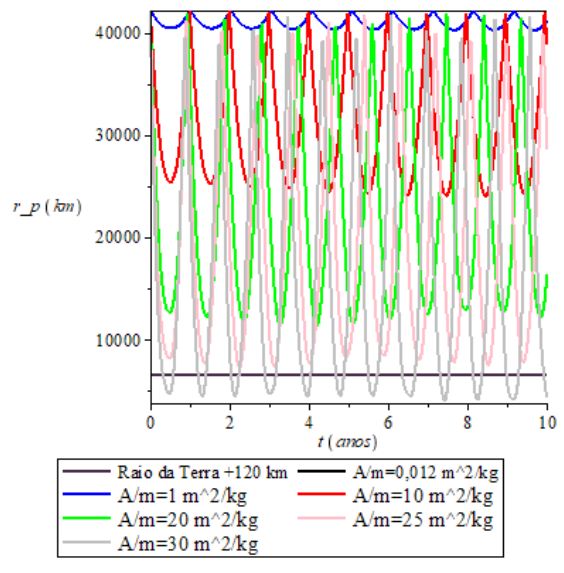
Figure 4 – (a) and time verses for different mass area values. (b) i versus time for different mass area values.



Source: Prepared by the authors

Figure 5 shows the position of the perigee, that is, the position of the satellite when it is closest to the Earth. For the value of A/m=25 the satellite approaches the re-entry region (horizontal line in violet) - region 120 km above the Earth's surface. For the value A/m=30 the satellite actually enters the atmospheric drag region and, in this way, the object will be incinerated during reentry. This is the purpose of using the solar sail, to direct the satellite so that it can re-enter the Earth's atmosphere to be incinerated.

Figure 5 – Position of the perigee (r_p) verses time for different values of mass area. From celestial mechanics we have to $r_p = a(1 - e)$



Source: Prepared by the authors

6.2 SIMULATION 2 - SATELLITE DECOMMISSIONED (SPACE DEBRIS)

INTELSAT I, was the first commercial communications satellite placed in geosynchronous Earth orbit on April 6, 1965, until it was decommissioned in January 1969 and has been in inactive orbit (space junk) ever since. Orbital data were obtained from site



https://www.privateer.com/. Orbital data: a=42170.3 km, e=0.0006, i=3.8038 degrees, Ω =85.9517 degrees, and w=65.9046 degrees. Comparing the orbital data of the case of simulation 2 with simulation 1, note that in the case of simulation 2, these data are slightly different from case 1, here the inclination was raised to i=3.8038, because in the geosynchronous orbit the inclination and eccentricities are almost zero. In this case, Figures 6(a) and (b) show a behavior similar to that of Figures 4 (a) and (b). In general, the satellites or debris that are in the GEO region behave in a similar way, these objects can remain in orbit for hundreds of years, see figure 3(a) in Carvalho, Vilhena de Moraes and Prado (2022), so to carry out the mitigation process it is necessary to use propulsion to remove the debris from the GEO region. In the case presented here, we use the solar sail as a propellant mechanism that uses the Sun's own energy source, which can contribute to the cleaning of the space environment in a sustainable way.

0.9 - 0.8 - 0.7 - 0.6 - 0.5 - 0.4 - 0.1 - 0.1 - 0.1 - 0.1 - 0.1 - 0.1 - 0.1 - 0.1 - 0.1 - 0.1 - 0.1 - 0.1 - 0.1 - 0.1 - 0.1 - 0.1 - 0.1 - 0.1 - 0.1 - 0.1 - 0.1 - 0.1 - 0.1 - 0.1 - 0.1 - 0.1 - 0.1 - 0.1 - 0.1 - 0.1 - 0.1 - 0.1 - 0.1 - 0.1 - 0.1 - 0.1 - 0.1 - 0.1 - 0.1 - 0.1 - 0.1 - 0.1 - 0.1 - 0.1 - 0.1 - 0.1 - 0.1 - 0.1 - 0.1 - 0.1 - 0.1 - 0.1 - 0.1 - 0.1 - 0.1 - 0.1 - 0.1 - 0.1 - 0.1 - 0.1 - 0.1 - 0.1 - 0.1 - 0.1 - 0.1 - 0.1 - 0.1 - 0.1 - 0.1 - 0.1 - 0.1 - 0.1 - 0.1 - 0.1 - 0.1 - 0.1 - 0.1 - 0.1 - 0.1 - 0.1 - 0.1 - 0.1 - 0.1 - 0.1 - 0.1 - 0.1 - 0.1 - 0.1 - 0.1 - 0.1 - 0.1 - 0.1 - 0.1 - 0.1 - 0.1 - 0.1 - 0.1 - 0.1 - 0.1 - 0.1 - 0.1 - 0.1 - 0.1 - 0.1 - 0.1 - 0.1 - 0.1 - 0.1 - 0.1 - 0.1 - 0.1 - 0.1 - 0.1 - 0.1 - 0.1 - 0.1 - 0.1 - 0.1 - 0.1 - 0.1 - 0.1 - 0.1 - 0.1 - 0.1 - 0.1 - 0.1 - 0.1 - 0.1 - 0.1 - 0.1 - 0.1 - 0.1 - 0.1 - 0.1 - 0.1 - 0.1 - 0.1 - 0.1 - 0.1 - 0.1 - 0.1 - 0.1 - 0.1 - 0.1 - 0.1 - 0.1 - 0.1 - 0.1 - 0.1 - 0.1 - 0.1 - 0.1 - 0.1 - 0.1 - 0.1 - 0.1 - 0.1 - 0.1 - 0.1 - 0.1 - 0.1 - 0.1 - 0.1 - 0.1 - 0.1 - 0.1 - 0.1 - 0.1 - 0.1 - 0.1 - 0.1 - 0.1 - 0.1 - 0.1 - 0.1 - 0.1 - 0.1 - 0.1 - 0.1 - 0.1 - 0.1 - 0.1 - 0.1 - 0.1 - 0.1 - 0.1 - 0.1 - 0.1 - 0.1 - 0.1 - 0.1 - 0.1 - 0.1 - 0.1 - 0.1 - 0.1 - 0.1 - 0.1 - 0.1 - 0.1 - 0.1 - 0.1 - 0.1 - 0.1 - 0.1 - 0.1 - 0.1 - 0.1 - 0.1 - 0.1 - 0.1 - 0.1 - 0.1 - 0.1 - 0.1 - 0.1 - 0.1 - 0.1 - 0.1 - 0.1 - 0.1 - 0.1 - 0.1 - 0.1 - 0.1 - 0.1 - 0.1 - 0.1 - 0.1 - 0.1 - 0.1 - 0.1 - 0.1 - 0.1 - 0.1 - 0.1 - 0.1 - 0.1 - 0.1 - 0.1 - 0.1 - 0.1 - 0.1 - 0.1 - 0.1 - 0.1 - 0.1 - 0.1 - 0.1 - 0.1 - 0.1 - 0.1 - 0.1 - 0.1 - 0.1 - 0.1 - 0.1 - 0.1 - 0.1 - 0.1 - 0.1 - 0.1 - 0.1 - 0.1 - 0.1 - 0.1 - 0.1 - 0.1 - 0.1 - 0.1 - 0.1 - 0.1 - 0.1 - 0.1 - 0.1 - 0.1 - 0.1 - 0.1 - 0.1 - 0.1 - 0.1 - 0.1 - 0.1 - 0.1 - 0.1 - 0.1 - 0.1 - 0.1 - 0.1 - 0.1 - 0.1 - 0.1 - 0.1 - 0.1 - 0.1 - 0.1 - 0.1 - 0.1 - 0.1 - 0.1 - 0.1 - 0.1 - 0.1 - 0.1 - 0.1 - 0.1 - 0.1 - 0.1 - 0.1 - 0.1 - 0.1 - 0.1 - 0.1 - 0.1 - 0.1 - 0.1 - 0.1 - 0.1 - 0.1 - 0.1 - 0.1 - 0.1 - 0.1 - 0.1 - 0.1 - 0.1 - 0.1 - 0.1 - 0.1 - 0.1 - 0.1 - 0.1 - 0.1 - 0.1 - 0.1 -

Figure 6 - (a) and time verses for different mass area values. (b) *i* versus time for different mass area values.

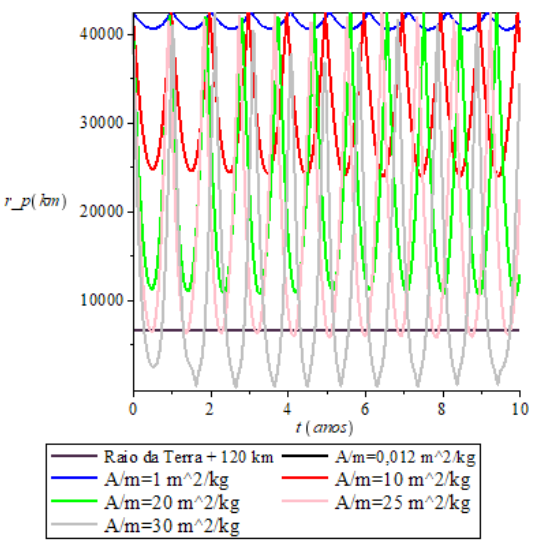
Source: Prepared by the authors

6.3 SIMULATION 3 - SATELLITE DECOMMISSIONED (SPACE DEBRIS)

INTELSAT 704, is a decommissioned satellite that was sent into a graveyard orbit, a region above GEO. Orbital data were obtained from site https://www.privateer.com/. Orbital data: a=42474.6 km, e=0.0015, i=9.4498 degrees, $\Omega=45.8469$ degrees and w=86.1365 degrees. Note that the initial conditions are slightly different from the previous cases, now the semi-major axis, eccentricity, and inclination have been changed to put the debris into a graveyard orbit using some propulsion mechanism. If we increase the area of the debris by attaching a solar sail, we notice that, in this case, with the value of A/m=25 the debris reaches the reentry region (see Figure 7), different from what happened in the case of simulation 1, just compare Figures 5 and 7.



Figure 7 – Position of the perigee (r_p) versus time for different values of mass area. From celestial mechanics we have to $r_p = a(1 - e)$



Source: Prepared by the authors

Finally, we show that with the help of a solar sail we can make the eccentricity of the debris be amplified so that the object approaches the re-entry region to be incinerated in the Earth's atmosphere. Analyzing the initial conditions of simulation 3, which shows the data of a debris in a cemetery orbit, we can conclude that with a small solar sail it is also possible to do the mitigation process by raising the debris to a cemetery orbit.

7 CONCLUSIONS

In this work, we analyze the characteristics of space debris orbiting the Earth. We present an analysis of ESA's 2022 annual report in which data regarding the amount of debris in different types of orbits are explored. We comment on the causes and consequences of these objects that after their useful life become a problem for space missions and the space environment. The ESA report comments on the need to create a subset of internationally accepted space debris mitigation measures and proposes to encourage sustainable missions and measures to address the global problem of space debris, it is up to nations, operators and individual manufacturers, to implement efforts to make near-Earth space sustainable in the long term. We mathematically model the main forces acting on the orbit of space debris, namely solar radiation pressure, flattening at the Earth's poles, and perturbation of the third body. We integrated the equations of motion obtained via Maple software, using the orbital data of real debris obtained from the https://www.privateer.com/ site. We use the solar sail to carry out the space debris mitigation process sustainably. We have shown that it is possible to use the solar sail for the removal of space debris, either by amplifying the eccentricity to force the debris to re-enter the Earth's atmosphere or by directing it into a graveyard orbit.

7

REFERENCES

- 1. Arshad, M., Bazzocchi, M. C. F., & Hussain, F. (2025). Emerging strategies in close proximity operations for space debris removal: A review. Acta Astronautica, 228, 996–1022. https://doi.org/10.1016/j.actaastro.2024.09.006
- 2. Carvalho, J. P., Lima, J. S., & Gonçalves, C. M. (2021). Poluição do ambiente espacial: O problema do lixo no espaço. Revista Scientia, 6(2), 61–80.
- 3. Carvalho, J. P. S., Vilhena de Moraes, R., & Prado, A. F. B. A. (2022). Analysis of the orbital evolution of space debris using a solar sail and natural forces. Advances in Space Research, 70(1), 125–143. https://doi.org/10.1016/j.asr.2022.04.013
- 4. Casanova, D., Petit, A., & Lemaître, A. (2015). Long-term evolution of space debris under the J2 effect, the solar radiation pressure and the solar and lunar perturbations. Celestial Mechanics and Dynamical Astronomy, 123(3), 223–238. https://doi.org/10.1007/s10569-015-9636-8
- 5. Cassen, R. (1987). Our common future: Report of the World Commission on Environment and Development. JSTOR. https://sustainabledevelopment.un.org/content/documents/5987our-commonfuture.pdf
- 6. European Space Agency. (2022). ESA's annual space environment report. https://www.sdo.esoc.esa.int/environment_report/Space_Environment_Report_latest. pdf
- 7. Ferreira, B. M. (2019). Técnicas e métodos de redução de detritos espaciais: Aplicação para uma vela solar [Unpublished bachelor's thesis]. Universidade Federal do Recôncavo da Bahia.
- 8. Formiga, J. K. S., Santos, D. P. S., Fiore, F. A., & Others. (2019). Study of collision probability considering a non-uniform cloud of space debris. Computational and Applied Mathematics, 39(1), Article 1. https://doi.org/10.1007/s40314-019-0994-3
- 9. Früh, C., & Jah, M. K. (2014). Coupled orbit attitude motion of high area-to-mass ratio (HAMR) objects including efficient self-shadowing. Acta Astronautica, 95, 227–241. https://doi.org/10.1016/j.actaastro.2013.11.017
- 10. Gkolias, I., & Colombo, C. (2019). Towards a sustainable exploitation of the geosynchronous orbital region. Celestial Mechanics and Dynamical Astronomy, 131(4), Article 19. https://doi.org/10.1007/s10569-019-9900-2
- 11. Gonçalves, C. M. (2021). Detrito espacial: Causas e consequências no ambiente espacial e terrestre [Unpublished bachelor's thesis]. Universidade Federal do Recôncavo da Bahia.
- 12. Hu, Y. P., Li, K. B., Wei, X., & Others. (2016). A novel space-based observation strategy for GEO objects based on daily pointing adjustment of multi-sensors. Advances in Space Research, 58(4), 505–513. https://doi.org/10.1016/j.asr.2016.05.012
- 13. Kelly, P., Erwin, R. S., Bevilacqua, R., & Others. (2016). Solar radiation pressure applications on geostationary satellites. In Proceedings of the 2016 AAS 16-012 Conference (pp. 1–12). American Astronautical Society.
- 14. Kessler, D. J., & Cour-Palais, B. G. (1978). Collision frequency of artificial satellites: The creation of a debris belt. Journal of Geophysical Research: Space Physics, 83(A6), 2637–2646. https://doi.org/10.1029/JA083iA06p02637
- 15. Lima, J. S. (2019). Uso da vela solar e das perturbações orbitais naturais para remoção de detritos espaciais [Unpublished bachelor's thesis]. Universidade Federal do Recôncavo da Bahia.
- 16. McInnes, C. R. (1999). Solar sailing: Technology, dynamics and mission applications. Springer-Verlag.
- 17. Murray, C. D., & Dermott, S. F. (1999). Solar system dynamics. Cambridge University Press.



- 18. Tresaco, E., Elipe, A., & Carvalho, J. P. S. (2016). Frozen orbits for a solar sail around Mercury. Journal of Guidance, Control, and Dynamics, 39(7), 1659–1666. https://doi.org/10.2514/1.G001477
- 19. Tresaco, E., Carvalho, J. P. S., Prado, A. F. B. A., & Others. (2018). Averaged model to study long-term dynamics of a probe about Mercury. Celestial Mechanics and Dynamical Astronomy, 130(2), Article 14. https://doi.org/10.1007/s10569-017-9802-6
- 20. Vilhena de Moraes, R. (1981). Combined solar radiation pressure and drag effects on the orbits of artificial satellites. Celestial Mechanics, 25(3), 281–292. https://doi.org/10.1007/BF01228944